

# THIN LIQUID FILMS FLOWING DOWN HEATED WALLS: A REVIEW OF RECENT RESULTS

*L. A. Dávalos-Orozco*

*Instituto de Investigaciones en Materiales, Departamento de Polímeros, Universidad Nacional Autónoma de México, Ciudad Universitaria, Circuito Exterior S/N, Delegación Coyoacán, 04510 México D. F., México, E-mail: ldavalos@unam.mx*

*Here a review is presented about the stability problem of thin liquid films flowing down heated walls. The period reviewed starts from 2013, after the publication of the extensive review paper by Dávalos-Orozco [Interfacial Phenom. Heat Transfer, vol. 1, pp. 93–138 (2013)]. Emphasis is given to flows where the film is affected by thermocapillarity under different mechanical and thermal boundary conditions. The subjects under discussion include thin films flowing down heated flat and cylindrical walls. Besides, the results on non-uniformly heated films are considered for flows under three different boundary situations: (1) temperature gradient along the wall, (2) local heating (hot plates), and (3) wall topography. Finally, pure experimental research papers are also taken into account in this review. The formation and separation of rivulets are examined along with their local increase of maximum thickness with distance down a hot plate.*

**KEY WORDS:** *thin liquid film, inclined plane, Marangoni effect, thermocapillarity*

## 1. INTRODUCTION

Thin liquid films have been the subject of extensive research due to their wide range of applications in industry. Theoretically it is a challenging area of investigation because one or more of their boundary conditions are unknown and they are part of the problem. Those boundary conditions correspond to free surface deformations and to interfacial deformations in case the liquid layer is stratified like in a two-layer or three-layer system. Therefore, mathematical models are needed to describe those free surface and interface boundary conditions. The linear and nonlinear evolution of those deformations are important to predict if the liquid film will wet the substrate or not after some interval of time.

When a horizontal wall is hot in comparison to the temperature of the atmosphere, the free surface of the liquid film presents perturbation patterns which differ from those corresponding to the isothermal case. In particular, the free surface corrugations increase when the temperature difference increases. This is a consequence of the temperature dependence of surface tension which generates tangential shear stresses on the free surface. Theoretically, the effect of these stresses is taken into account in extra non-linear terms included in the free surface nonlinear evolution equation. It can be shown that when the wall is a very good conductor, these terms are destabilizing and that the increase of the temperature gradient increases the amplitude of the free surface perturbations in comparison with the isothermal flow. Furthermore, large temperature gradients may lead to the formation of holes (dewetting) in the liquid film when the amplitude of the perturbations equals the mean film thickness.

When the wall is inclined with respect to the horizontal direction, the liquid film feels the pull of gravity down the wall and forms a main flow velocity profile. This flow can be unstable under isothermal conditions. The presence of a temperature gradient across the film can modify this instability (Dávalos-Orozco, 2013). In this case, the increase of the temperature gradient may lead to the formation of rivulets and to intense evaporation. The film might not be able to wet the substrate if the temperature gradient is increased considerably.

This paper is devoted to present a review of research done on the problem discussed in the last paragraph, that is, the thermocapillary instability of thin films falling down hot walls. The period under review is from 2013 to date, just after the publication of the extensive review paper by Dávalos-Orozco (2013). The next section presents a sketch of a

### NOMENCLATURE

<p><math>A</math> air jet maximum time dependent pressure</p> <p><math>a</math> air jet time dependent pressure dispersion</p> <p><math>Bi</math> Biot number</p> <p><math>d</math> <math>d_{wall}/h_0</math></p> <p><math>d_{wall}</math> wall thickness</p> <p><math>h(x,y,t)</math> film local thickness</p> <p><math>H(x,y,t)</math> film local perturbation</p> <p><math>h_0</math> unperturbed film thickness</p> <p><math>H_h</math> heat transfer coefficient</p> <p><math>k_f</math> fluid heat conductivity</p> <p><math>k_{wall}</math> wall heat conductivity</p> <p><math>L</math> wall wavelength over perturbations wavelength ratio</p> <p><math>Ma</math> Marangoni number</p> <p><math>p</math> pressure</p> <p><math>P_p</math> surface external pressure</p> <p><math>Pr</math> Prandtl number</p> <p><math>Q_c</math> wall over fluid conductivities ratio</p> <p><math>R</math> Reynolds number</p> <p><math>S</math> scaled surface tension number</p> <p><math>T</math> fluid temperature</p>	<p><math>T_{ambient}</math> ambient atmosphere temperature</p> <p><math>T_L</math> wall lower face temperature</p> <p><math>T_{wall}</math> wall temperature</p> <p><math>T_{wall0}</math> zeroth-order wall temperature</p> <p><math>T_0</math> zeroth-order fluid temperature</p> <p><math>u</math> velocity x component</p> <p><math>v</math> velocity y component</p> <p><math>w</math> velocity z component</p> <p><b>Greek Symbols</b></p> <p><math>\beta</math> wall inclination angle</p> <p><math>\Delta</math> means difference</p> <p><math>\varepsilon</math> wave slope smallness parameter</p> <p><math>\zeta</math> wall deformation</p> <p><math>\kappa</math> thermal diffusivity</p> <p><math>\lambda</math> wavelength</p> <p><math>\nu</math> kinematic viscosity</p> <p><math>\rho</math> fluid density</p> <p><math>\sigma</math> surface tension</p> <p><math>\Sigma</math> surface tension number</p> <p><math>\omega</math> frequency of oscillation</p>
---	---

more general system, that of a thin film flowing down a thick and wavy wall. This section also includes a description of the general system of equations of motion and heat transfer with the corresponding boundary conditions. The areas of the papers discussed are distributed as in the following sections. Section 3 presents flows on flat walls. Section 4 is devoted to flows down cylinders. Then, problems of non-uniform heating are presented in Section 5, which is divided in to three parts: first, flow down a wall with a longitudinal temperature gradient, second, flow down a wall with a finite hot plate, and third, flow down a wall with topography. Some experiments are discussed in Section 6. Finally, the conclusions are given in Section 7.

## 2. SYSTEM DESCRIPTION, EQUATIONS, AND BOUNDARY CONDITIONS

The liquid films discussed here are falling down heated walls which can be flat, wavy, or cylindrical. In the case of a wavy wall a general vertical system is described in Fig. 1. In the figure a thin film with non-dimensional thickness 1 is flowing down a vertical thick wall which has wavy deformations around a mean non-dimensional thickness  $d$ . Despite the waviness, the thickness of the wall is never zero. Due to the wall deformations the free surface has a response which depends on the parameters of the problem like surface tension and Reynolds number. Besides, time-dependent perturbations are applied at the origin ( $x = 0$ ) above the free surface. They propagate down the free surface response. It is assumed that the temperatures below the lower side of the wall and the atmosphere above the free surface are different. Therefore, the liquid film is susceptible to thermocapillary instabilities due to the changes the surface tension has with respect to temperature. These changes generate tangential shear stresses that lead to more free surface instabilities, which are the subject of the present review.

The equations of motion, continuity, and heat diffusion in the fluid and the wall in non-dimensional form are

$$\varepsilon u_t + \varepsilon u u_x + \varepsilon v u_y + w u_z = -\varepsilon p_x + \varepsilon^2 u_{xx} + \varepsilon^2 u_{yy} + u_{zz} + R \sin \beta, \quad (1)$$

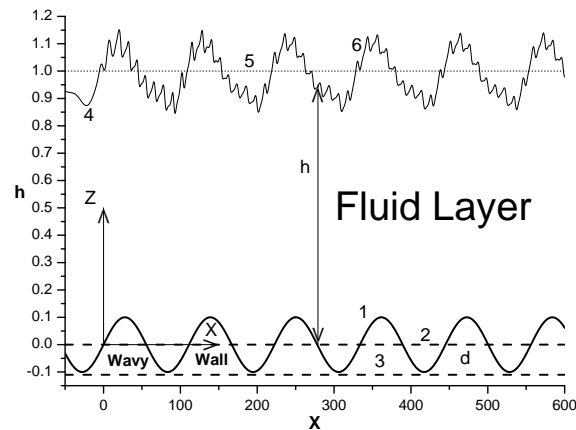


**FIG. 1:** Vertical wall and thin film system. (1) Wall sinusoidal deformation (solid), (2) Mean height of the wall (dashed) with thickness  $d$ , (3) Lower side of the wall (dashed), (4) Free surface response to the wall deformation, (5) Mean height of the unperturbed free surface (dotted), (6) Time-dependent perturbations excited at  $x = 0$  and running on the free surfaces response. They have a local height  $h(x,t)$  with respect to the wall deformation. The wall has a largest and smallest (not zero) thicknesses.

$$\varepsilon v_t + \varepsilon u v_x + \varepsilon v v_y + w v_z = -\varepsilon p_y + \varepsilon^2 v_{xx} + \varepsilon^2 v_{yy} + v_{zz}, \quad (2)$$

$$\varepsilon w_t + \varepsilon u w_x + \varepsilon v w_y + w w_z = -p_z + \varepsilon^2 w_{xx} + \varepsilon^2 w_{yy} + w_{zz} - R \cos \beta, \quad (3)$$

$$w_z = -\varepsilon u_x - \varepsilon v_y, \quad (4)$$

$$\text{Pr} (\varepsilon T_t + \varepsilon u T_x + \varepsilon v T_y + w T_z) = \varepsilon^2 T_{xx} + \varepsilon^2 T_{yy} + T_{zz}. \quad (5)$$

$$\frac{\nu}{k_{wall}} \varepsilon T_{wallt} = \varepsilon^2 T_{wallxx} + \varepsilon^2 T_{wallyy} + T_{wallzz}. \quad (6)$$

Subindexes  $x, y, z$ , and  $t$  mean partial derivatives. The velocity components are  $(u, v, w)$  in the  $(x, y, z)$  directions,  $p$  is the pressure,  $T$  is the temperature,  $T_{wall}$  is the wall temperature, and  $k_{wall}$  is the wall thermal diffusivity.

The equations were made non-dimensional by means of  $h_0$ , the mean thickness of the liquid layer, for distance in the  $z$  direction,  $\lambda/2\pi$  for distance in the  $x$ - and  $y$ -directions,  $h_0\lambda/(\nu 2\pi)$  for time, where  $\lambda$  is a representative length of the free surface deformation.  $\nu/h_0$  is used for velocity,  $\rho\nu^2/h_0^2$  for pressure, and  $\Delta T = T_L - T_{ambient} > 0$  for temperature. Here,  $\nu$  is the kinematic viscosity and  $\rho$  is the density. In the above temperature difference,  $T_L$  is the temperature at the lower face of the wall and  $T_{ambient}$  is the temperature of the ambient atmosphere above the fluid free surface. Notice that a scaling parameter  $\varepsilon = 2\pi h_0/\lambda \ll 1$  has been used. It means that the slope of the free surface perturbations is small and that it will be used as a reference to make an asymptotic expansion of the variables of the problem. In the equations the angle of inclination of the wall is  $\beta$ , the Reynolds number  $R = gh_0^3/\nu^2$ , and the Prandtl number is  $\text{Pr} = \nu/\kappa$ , where  $\kappa$  is the fluid thermal diffusivity. Let the wall surface be located at  $z = \zeta(x, y)$  where  $\zeta(x, y)$  is a general wall profile assumed here as sinusoidal [see Dávalos-Orozco (2007)]. Then the unperturbed free surface is located at  $z = \zeta(x, y) + 1$ . In the absence of time-dependent perturbations the response of the free surface to the wall deformation is  $z = \zeta(x, y) + 1 + H(x, y, t) = \zeta(x, y) + h(x, y, t)$ , with  $h(x, y, t) = 1 + H(x, y, t)$ . The addition of time-dependent perturbations will modify  $H(x, y, t)$ , as can be seen in Fig. 1.

The boundary conditions needed to solve the above equations are as follows. At the wall, the non-slip boundary condition is

$$u = v = w = 0 \quad \text{at} \quad z = \zeta(x, y), \quad (7)$$

When the wall is flat  $\zeta(x, y) = 0$ . The normal stress boundary condition is

$$\begin{aligned} & -p + \frac{1}{N^2} [\varepsilon^3(u_x f_x^2 + v_y f_y^2) + \varepsilon^3(u_y + v_x) f_x f_y - \varepsilon(v_z + \varepsilon w_y) f_y - \varepsilon(u_z + \varepsilon w_x) f_x + w_z] \\ & = P_p(x, y, t) - \frac{3}{N^3} S [(1 + \varepsilon^2 f_y^2) f_{xx} + (1 + \varepsilon^2 f_x^2) f_{yy} - 2\varepsilon^2 f_x f_y f_{xy}] \quad \text{at} \quad z = \zeta(x, y) + h(x, y, t), \end{aligned} \quad (8)$$

where it is convenient to define  $f(x, y, t) = \zeta(x, y) + h(x, y, t)$  and  $N = \sqrt{1 + \varepsilon^2 f_x^2 + \varepsilon^2 f_y^2}$ . The balance of tangential shear stresses due to the gradients of surface tension with respect to temperature are the first shear stress boundary condition:

$$\begin{aligned} & \varepsilon(w_z - \varepsilon u_x) f_x - \frac{1}{2} \varepsilon^2 (u_y + v_x) f_y + \frac{1}{2} (u_z + \varepsilon w_x) (1 - \varepsilon^2 f_x^2) \\ & - \frac{1}{2} \varepsilon^2 (\varepsilon w_y + v_z) f_x f_y = \frac{\text{Ma}}{\text{Pr}} (\varepsilon T_x + \varepsilon h_x T_z) \quad \text{at} \quad z = \zeta(x, y) + h(x, y, t), \end{aligned} \quad (9)$$

and the second shear stress boundary condition:

$$\begin{aligned} & \varepsilon(w_z - \varepsilon u_y) f_y - \frac{1}{2} \varepsilon^2 (u_y + v_x) f_x + \frac{1}{2} (v_z + \varepsilon w_y) (1 - \varepsilon^2 f_y^2) \\ & - \frac{1}{2} \varepsilon^2 (\varepsilon w_x + u_z) f_x f_y = \frac{\text{Ma}}{\text{Pr}} (\varepsilon T_y + \varepsilon h_y T_z) \quad \text{at} \quad z = \zeta(x, y) + h(x, y, t). \end{aligned} \quad (10)$$

The boundary conditions for the temperature are

$$\begin{aligned} & T_{wall} = 1, \quad \text{at} \quad z = -d \\ & T_{wall} = T \quad \text{and} \quad Q_c dT_{wall}/dz = dT/dz, \quad \text{at} \quad z = 0 \\ & T_z + \text{Bi} T = 0 \quad \text{at} \quad z = \zeta(x, y) + h(x, y, t), \end{aligned} \quad (11)$$

where  $S = \varepsilon^2 \Sigma$  and  $\Sigma = \sigma h_0 / (3\rho v^2)$  is a scaled surface tension number, used for strong surface tension fluids, and  $\sigma$  the surface tension. The ratio of the wall and fluid heat conductivities is represented by  $Q_c = k_{wall}/k_f$ . The Biot number is  $\text{Bi} = H_h h_0 / k_f$  and  $H_h$  is the coefficient of heat transfer. The Marangoni number is defined as  $\text{Ma} = (-d\sigma/dT) \Delta T h_0 / (\rho v \kappa)$ . The condition that a fluid particle on the free surface remains on the free surface as time evolves is the kinematic boundary condition:

$$w = \varepsilon h_t + \varepsilon u f_x + \varepsilon v f_y \quad \text{at} \quad z = \zeta(x, y) + h(x, y, t). \quad (13)$$

A pressure distribution  $P_p(x, y, t)$  appears in the normal stress boundary condition Eq. (8), which is used to apply time-dependent perturbation on the free surface [see Dávalos-Orozco (2007, 2014, 2015)]. It allows control of the frequency of the perturbations and consequently their wavenumber.

Now, the variables are expanded as

$$\begin{aligned} & u = u_0 + \varepsilon u_1 + \dots, \quad v = v_0 + \varepsilon v_1 + \dots, \quad w = \varepsilon(w_1 + \varepsilon w_2 + \dots), \\ & p = p_0 + \varepsilon p_1 + \dots, \quad T = T_0 + \varepsilon T_1 + \dots, \quad T_{wall} = T_{wall0} + \varepsilon T_{wall1} + \dots. \end{aligned} \quad (14)$$

The above expansions are used in the equations of motion, continuity, heat diffusion, and boundary conditions. Here, due to its importance, only the results for the main temperature profiles are presented. They are

$$T_{w0} = \frac{Q_C (1 + \text{Bi} h(x, y, t)) - \text{Bi} (z - \zeta(x, y))}{Q_C (1 + \text{Bi} h(x, y, t)) + \text{Bi} (d + \zeta(x, y))}, \quad (15)$$

$$T_0 = \frac{Q_C (1 + \text{Bi} h(x, y, t)) - \text{Bi} Q_C (z - \zeta(x, y))}{Q_C (1 + \text{Bi} h(x, y, t)) + \text{Bi} (d + \zeta(x, y))}. \quad (16)$$

Notice that  $T_{w0}$  equals one at  $-d$  and equals  $T_0$  at  $z = \zeta(x, y)$ . The heat flux boundary condition is also satisfied at  $z = \zeta(x, y)$ . At the lowest order the free surface deformation satisfies

$$h_t = -R \sin \beta h^2 \frac{\partial h}{\partial x} \quad \text{at} \quad z = \zeta(x, y) + h(x, y, t). \quad (17)$$

At the next order, the result is an evolution equation of the Benney type for the free surface deformation of a thin film flowing down an inclined thick wall with smooth deformations. That is,

$$\begin{aligned} h_t + R \sin \beta h^2 h_x + \varepsilon \left\{ (R \sin \beta)^2 \left( \frac{2}{15} h^6 h_x \right)_x + \frac{1}{3} \nabla \cdot \left[ h^3 (-R \cos \beta \nabla (\zeta + h)) \right. \right. \\ \left. \left. + 3S \nabla^2 \nabla (\zeta + h) - \nabla P_p \right] + \frac{3 \text{Ma}}{2 \text{Pr}} \frac{\text{Bi} h^2 \left[ \nabla h + \frac{1}{Q_C} \nabla \zeta \right]}{\left( 1 + \text{Bi} \left[ h + \frac{1}{Q_C} \zeta + \frac{d}{Q_C} \right] \right)^2} \right\} = 0. \end{aligned} \quad (18)$$

Here,  $\nabla = (\partial/\partial x, \partial/\partial y)$  is the horizontal nabla operator. It is clear that when  $\zeta(x, y) = 0$  this equation reduces to that obtained by Dávalos-Orozco (2012). However, when  $Q_C \rightarrow \infty$  (very good conducting wall) this equation reduces to equation (A3) in the appendix of D'Alessio et al. (2010). Notice that there the wall deformation is missing in the thermocapillary term. In the same limit but when the wall is flat  $\zeta = 0$  and  $\text{Ma} = 0$ , the equation reduces to a perturbed Benney equation (Dávalos-Orozco et al., 1997). Moreover, if also  $P_p = 0$  the equation reduces to that of Benney (1966) (see also Joo et al., 1991; Joo and Davis, 1996). In the case  $P_p = 0$  and  $\text{Ma} > 0$  the equation reduces to that used by Joo et al. (1991) when their evaporation number  $E = 0$  (no evaporation). They use a parameter  $K$  which is  $1/\text{Bi}$ , the inverse of the Biot number.

The smoothness required by the wall deformations becomes clear from Eq. (18) where  $\zeta(x, y)$  must have continuous derivatives up to the fourth order. This restriction is satisfied by a sinusoidal function. In some of the papers reviewed below where the lubrication approximation is assumed, a simplified version of Eq. (18) is used, but with additional terms corresponding to the problem investigated.

### 3. THIN FILMS FLOWING DOWN HEATED FLAT WALLS

This section is devoted to the stability of liquid films flowing down non-deformed walls which are heated uniformly. In this way, it is also assumed that the temperature distribution of the atmosphere on the other side of the film is uniform too. The results of the papers are mainly theoretical but in one case theoretical and experimental results are presented simultaneously.

Flows of thin films flowing down walls including buoyancy effects have been investigated in two publications. First, Pascal et al. (2013) assume that all the physical properties of the fluid are temperature dependent in a linear way and therefore they also include the variation of the density except in front of the time Lagrange operator, like in the Boussinesq approximation. The equations of motion and heat transfer are more complex than those in Eqs. (1)–(6) and corresponding boundary conditions. The reason is that new terms appear with the spatial derivatives of the physical properties and the buoyancy term. These derivatives are translated into temperature derivatives of the physical properties. Notice that the variation of viscosity has been considered in the absence of Marangoni forces by Goussis and Kelly (1985, 1987) and Hwang and Weng (1988), and for a stationary flow by Kabova and Kuznetsov (2002). In this way, Pascal et al. (2013) investigate the linear stability of the film by means of a small wavenumber approximation. Under these conditions, the main velocity and temperature profiles have a very complicated algebraic expression. Therefore, a variety of main flow solutions are given making zero one or more of the parameters. With them, the critical Reynolds number is calculated for each case. In particular, it is shown that an increase in the viscosity temperature derivative is destabilizing due to an increase of inertia, and an increase in the density temperature derivative is stabilizing due to the decrease in density. The latter effect is shown in Fig. 2, for the particular parameters selected. There, the critical Reynolds number stabilizes increasing monotonically. However, its magnitude decreases destabilizing with the growth of the viscosity temperature derivative.

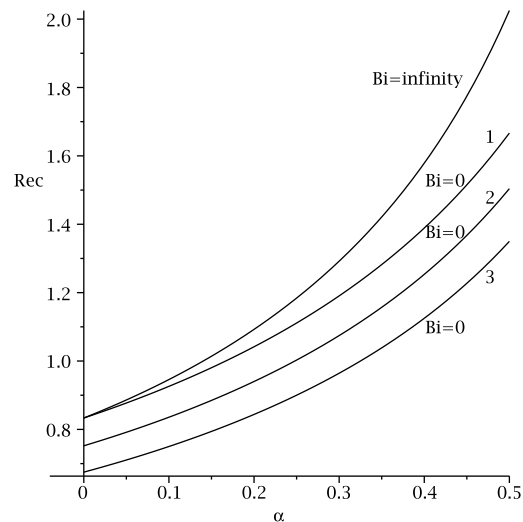


**FIG. 2:** Critical Reynolds number vs  $\alpha$  (density temperature derivative). The effects of buoyancy on a thin film flowing down a wall inclined 45 degrees. Two sample cases. (A) Biot number infinity, for zero thermal conductivity and viscosity temperature derivatives. (B) Biot number = 0, for heat capacity temperature derivative 0.1, relative temperature difference 0.1, and Prandtl number 10. Three magnitudes of the viscosity temperature derivative: (1) 0, (2) 0.05, and (3) 0.1.

Prokudina (2014a) calculates the linear and nonlinear stability of the free surface perturbations of a liquid film subjected to condensation or evaporation. Thermocapillary effects are also taken into account including surface viscosity which comes from the presence of surfactants. Previous work on this subject is found in Prokudina and Vyatkin (1998). By means of perturbation methods (see van Dyke, 1975) a model equation is calculated for the evolution of the free surface perturbations under the small wavenumber approximation. In the linear stability problem it is shown that the growth rate of the perturbation in the evaporation case is larger than that of the condensation one. The role of the surface viscosity is to reduce the growth rate mainly when the wavenumber is relatively large. The non-linear solutions show that the film thickness increases with condensation and decreases with evaporation. It is concluded that the increase of the temperature gradient adds extra corrugation to the film free surface.

D'Alessio et al. (2014) present a linear stability analysis where the critical Reynolds number is calculated including the full set of parameters coming from the temperature-dependent physical properties. They concentrate their attention on the stability behavior when the buoyancy term (related to the density) changes as in the Boussinesq approximation. They show that buoyancy has a dual role. When the buoyancy term increases, the thin film density decreases with a stabilizing effect. However, due to the density dependence on the coordinate perpendicular to the wall (through the main temperature profile), the density is larger near the free surface where it has a destabilizing effect by the promotion of surface deformation. In this problem, among other things, it is found that the phase velocity varies with the parameters. Figure 3 shows that it varies linearly with the density temperature gradient and changes with the Biot number fixing other parameters. It is independent from the Marangoni and Prandtl numbers but depends on the Biot number. The figure shows results for a magnitude of 0.5 for each the viscosity and thermal conductivity temperature derivatives.

Prokudina (2014b) investigates the propagation of wave packets on the free surface of a film flowing down a hot wall. The effects of condensation and evaporation are taken into account. The evolution of the free surface perturbations is described by means of a Ginzburg–Landau-type equation. This equation for thin films has been investigated previously for example by Prokudina and Vyatkin (2011). It is obtained by means of a multiple scales expansion method as explained in Nayfeh (1973). Here an envelope equation for a complex amplitude is calculated using the method by Elyukhin and Kalimulina (1979). For a vertical film, it is found in the nonlinear theory that for Reynolds

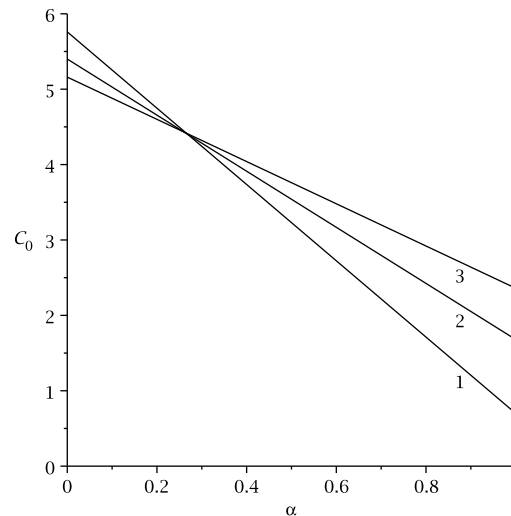


**FIG. 3:** Phase velocity vs  $\alpha$  (density temperature derivative). The effects of buoyancy on a thin film flowing down a wall. Three Biot numbers: (1) 0.25, (2) 1, (3) 3.

numbers smaller than 7 the phase velocity of the free surface perturbations depends linearly on the wave amplitude, but for Reynolds numbers larger than 7 it depends nonlinearly on the wave amplitude. Besides, it is shown that the surface viscosity produces a decrease in the amplitude of the nonlinear perturbation. Despite the three-dimensional character of the perturbations, it is demonstrated that longitudinal modes in the flow direction are the most unstable. Likewise, near criticality the energy of neighboring perturbations is transferred to those in the neighborhood of the maximum growth rate.

Quan et al. (2015) make experiments and numerical analysis related with the shrinkage of a thin film flowing down a wall with vapor counter flow. Notice that this is not a rivulet, it is a film with finite but wide width. It is found that while the heat transfer is enhanced, the shrinkage is reduced when the film temperature and flow rate are larger. This is seen in Fig. 4, where the width of the film, measured by experiment, is plotted against the distance from the inlet down to 0.4 m. The temperature at the inlet ranges from 30 degrees to 70 degrees Celsius. Numerical analysis on thin films focused on film rupture have been done by Joo et al. (1996), Kim (1999), Miladinova and Lebon (2005), and Zhang et al. (2008a,b). Here, these measurements are confirmed by numerical analysis which includes thermocapillary effects. Near the distance of 0.4 m a small difference is found. It seems that thermocapillarity is mainly responsible for the shrinkage of the film. As a side effect, it is found that the heat transfer decreases considerably. It is shown that the film is thicker at the edges in comparison to the middle section and the temperature there is higher too. These temperature differences are the source of the film shrinkage because they produce a shear flow by means of the temperature dependent surface tension.

Ding and Wong (2015) use a first-order weighted-residual method, first proposed by Ruyer-Quil and Manneville (2000, 2002), (see Dávalos-Orozco, 2013) to find a model evolution equation for the free surface perturbations on a thin film falling down a heated or cooled slippery wall. Besides, a Benney-type evolution equation is calculated in order to compare the results with those of the other model. In the two-dimensional case, instead of the wall boundary condition Eq. (7), use is made of the condition

$$u = l_S u_z \quad \text{and} \quad w = 0 \quad \text{at the wall,} \quad (19)$$

where  $l_S$  is the slippery length and the subindex in  $u$  means partial derivative. In case  $l_S = 0$  the fluid sticks to the wall. When  $l_S \rightarrow \infty$  then  $u_z \rightarrow 0$  and the wall is completely slippery (or the wall is absent). Under these conditions, the Benney-type evolution Eq. (18) should have an additional term  $l_S h^2$  inside the large brackets  $[\ ]$ . In the linear problem

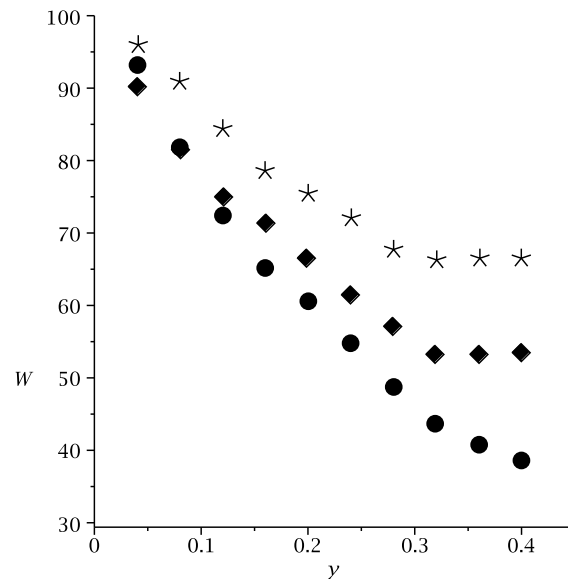


**FIG. 4:** Film width  $W$  vs distance  $y$  from the inlet. Temperature at the inlet: Solid circles  $30^\circ$ , solid diamonds  $50^\circ$ , and asterisks  $70^\circ$  Celsius.

they find that the results of the Benney model are limited to Reynolds numbers smaller than one. This conclusion was first obtained by Scheid et al. (2005) in the absence of slip on the wall. Besides, they investigate the influence of thermocapillarity and wall slip on the the nonlinear numerical solution of traveling waves. When the film is heated from the wall, free surface instabilities are promoted in the flow. The contrary is true when it is cooled from the wall. The film is more unstable when both inertia and slip parameter are large. Besides, it is found that the phase velocity increases with the slip parameter. From the nonlinear point of view, calculations show that the free surface perturbations increase with the slip parameter and thermocapillary effects.

#### 4. THIN FILMS FLOWING DOWN VERTICAL HEATED CYLINDERS

A common deviation from the geometry of a flat wall is that of a cylindrical substrate. Two approximations were investigated in the period under review. The first one is related to very thin cylindrical walls, the so-called fibers. The other one corresponds to cylinders with very large radius in comparison to the film thickness.

Liu and Liu (2014) investigate the formation of beads from thin films flowing down hot vertical fibers. The problem was investigated by Frenkel (1992), who calculated an evolution equation of the Benney type where the thickness of the film is assumed smaller than the radius of the fiber. The equation was solved by Kalliadasis and Chang (1994) and experiments have been done by Quere (1990). Liu and Liu (2014) calculate a nonlinear evolution equation under the approximation of very large capillary length scale with respect to the radius of the cylinder. The result is in agreement with a long wavelength approximation. The thermocapillary effects are due to a temperature gradient across the cylindrical liquid film coating the fiber. In the linear stability analysis it is found that an increase of the Marangoni number increases the growth rate and the wavenumber of the most unstable perturbation. This phenomenon occurs along with the throttling effect of surface tension in the radial direction. The maximum growth rate and the corresponding wavenumber also have maximum magnitude with respect to the Biot number. The Biot number corresponding to this maximum has a small displacement with the change of the radius of the fiber. In fact, it is pointed out the relevance the relation  $Bi = 1/\ln(1/a)$  has to attain the maximum value of the growth rate and the corresponding wavenumber, where  $a$  is the non-dimensional radius of the fiber. This can be seen in the expression of the maximum growth rate with respect to the wavenumber



$$\Gamma_{\max} = \frac{A}{64\varepsilon^2} E^2, \quad k_{\max} = \frac{1}{\sqrt{2\varepsilon}} E^{1/2}, \quad \text{where } E = \left( 1 + 4\varepsilon \text{Ma} \frac{\text{Bi}}{(\text{Bi} \ln a - 1)^2} \frac{B}{A} \right) \quad (20)$$

where  $\varepsilon$  here is the ratio of the radius of the fiber over the representative length scale and  $A = -4 \ln a - a^4 + 4a^2 - 3$  and  $B = (a^2 - 1 - 2 \ln a)(1 - \ln a)$ . This  $\Gamma_{\max}$  has also a maximum with respect to  $\text{Bi}$  with magnitude  $\text{Bi} = 1/\ln(1/a)$ . Notice that  $a < 1$ . It can be shown that  $k_{\max}$  has also a maximum at  $\text{Bi} = 1/\ln(1/a)$ . The numerical analysis of the nonlinear equation is done for both the most unstable perturbations and for random small perturbations. When the perturbations are the most unstable, it is found that saturation is faster with thermocapillary effects than in isothermal conditions. The height and separation of the beads are larger too. In the case of small random perturbations it is found that increasing the temperature gradient a row of beads is formed and that the film left between a pair of beads is thinner with a tendency to breakup. The film also presents traveling wave solutions where the long wavelength drops catch up with the short wavelength ones which eventually are swallowed.

Moctezuma-Sánchez and Dávalos-Orozco (2015) investigate the linear stability of a viscoelastic liquid film coating the outside of a heated cylinder in two cases: in the absence of gravity and the stability when the film flows down a heated vertical cylinder under the action of gravity. The calculations are made under the small wavenumber and large cylinder radius approximation. The problem has been investigated by Shlang and Sivashinsky (1982) and Frenkel (1993) in the isothermal case and by Moctezuma-Sánchez and Dávalos-Orozco (2008) for an isothermal viscoelastic fluid. The thermocapillary problem was first investigated including azimuthal modes by Dávalos-Orozco and You (2000). In Moctezuma-Sánchez and Dávalos-Orozco (2015) a linear partial differential equation is obtained to describe the three-dimensional stability of the free surface perturbations. The interest is to understand the stability of the axial and azimuthal modes under the influence of thermocapillary effects. It is found that viscoelasticity promotes the appearance of azimuthal modes by increasing their growth rate of instability. The results show that the axial mode is the most unstable one. However, it is demonstrated that the azimuthal modes can be the more unstable in a wide region of the wavenumber range. This is shown in Fig. 5 when the film falls down a hot cylinder due to gravity. As can be seen, the Reynolds number stabilizes the flow working to avoid the throttling instability in the radial direction. The azimuthal modes can be excited as the more unstable when external or ambient perturbations fall inside the

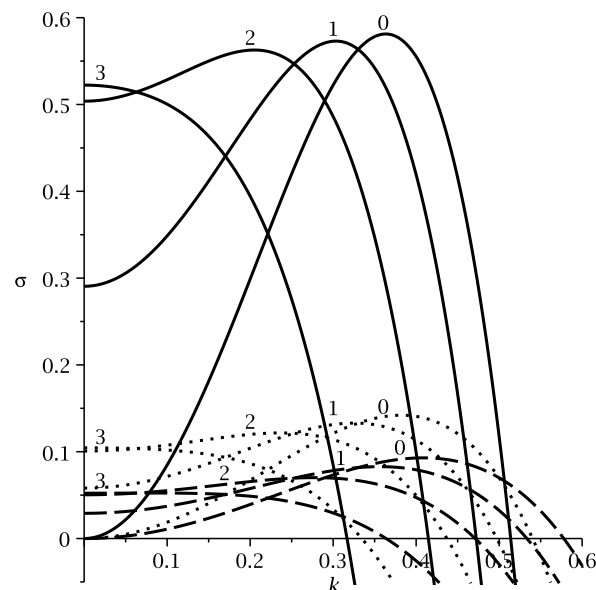


**FIG. 5:** Growth rate vs wavenumber.  $\text{Ma}/\text{Pr} = 2$ ,  $\text{Bi} = 0.1$ ,  $S = 1$ . Non-dimensional radius = 10, Deborah number = 0.2. Solid:  $R = 0.1$ , Dotted:  $R = 0.2$ , Dashed:  $R = 0.1$ . The numbers of the modes: axial mode: 0, azimuthal modes: 1, 2, 3.

corresponding wavenumber range (see Fig. 5) or by controlling the wavenumber of the free surface perturbation. An increase of the viscoelasticity parameter (the Deborah number), the Marangoni number, or the radius of the cylinder leads to the appearance of many azimuthal modes as the more unstable in a range of the wavenumber. In the example of Fig. 5 the distribution of the modes maxima of growth rate is ordered, from small to large wavenumbers, as mode 3, mode 2, mode 1, mode 0. In the figure, the absolute maximum is for mode 0 (the axial mode). However, in the range between  $k = 0$  and the intersection between modes 3 and 2, it is found that these two modes are very near each other, but the growth rate of the other two modes decreases very fast near to  $k = 0$ . Notice that mode 1 is always below but very near the axial mode 0. This occurs in almost all the thermocapillary cases investigated and might be important in the nonlinear problem.

## 5. THIN FILMS FLOWING DOWN NON-UNIFORMLY HEATED FLAT WALLS

The non-uniform heating will be discussed in three sections taking into account the temperature gradient along the flow direction and the geometry of the wall. First is the case where the temperature changes down the wall. Second is the situation where the wall is flat but the film is heated by an abrupt change in the temperature of the wall. The third corresponds to a wall heated uniformly but due to its geometric characteristics, like topography, the liquid film feels a non-uniform heating effect.

### 5.1 Temperature Gradient along the Wall

Bekezhanova and Rodionova (2015) investigate the (Ostroumov–Birikh-type) profiles of the main flow variables of a two-layer film flowing down an inclined hot wall subjected to buoyancy effects. The upper fluid film has a free surface. The problem of a two-layer film confined between two walls was investigated by Napolitano (1980) including thermocapillarity. A complete review of two-layer problems with Marangoni effect is presented in the monography by Nepomnyashchy et al. (2006). Some exact solutions were calculated by Birikh (1966). Previous research on the subject can be found in Bekezhanova (2011) who considers also the variations in the flow stability when the velocity profiles are changed. In Bekezhanova and Rodionova (2015) the atmosphere above the free surface has a different temperature from that of the wall. Also, the wall has a temperature gradient along the main flow direction. In other words, the two-layer film is subjected to an inclined temperature gradient. However, thermocapillary effects due to the wall-atmosphere temperatures difference are not taken into account. The buoyancy effects are assumed to be due only to the temperature gradient parallel to the wall. The flow stability is investigated assuming that the interface between the two fluids and the free surface of the upper fluid are flat. Stability calculations are done only for the two separate cases where gravity is zero and where the angle of inclination of the wall is zero. Though the results are of interest, these two cases are outside the scope of the present review. However, results of a variety of main velocity profiles are presented where the angles of inclination are different from zero.

### 5.2 Local Heating

Liu and Kabov (2013) investigate numerically the linear and nonlinear instability of a thin film flowing down a locally heated wall with square and rectangular heaters arranged one after the other in the flow direction. Previous research, experimental and numerical, has been done by Frank (2003), Frank and Kabov (2006), and Kabova et al. (2007). Liu and Kabov (2013) make the small wavenumber approximation for two- and three-dimensional perturbations. The two-dimensional problem implies that a heater in the form of an infinite band is placed in the wall. In that case a nonlinear steady-state flow appears which is unstable to large thermocapillary effects. In the three-dimensional problem the local heating is finite, as with square and rectangular heaters. It is found that for rectangular heaters the free surface deformations are linearly stable to thermocapillary effects and they form a steady and strong structure. The rupture of the film depends therefore on the thermal behavior of this strong structure which presents the thinnest part of the film downstream but near to the heater. In the case of two heaters, this thinnest part of the film is located downstream the second heater. Accordingly, it is concluded that the mutual location of the heaters is important on the stability of

the film. This is evident in Fig. 6, where the minimum thickness of the layer  $h_{\min}$  is plotted against the Marangoni number. It is shown that  $h_{\min}$  becomes zero for smaller Ma when two heaters are present.

Ding and Wong (2013) investigate the stability of a thin film falling down a wall locally heated which presents at the free surface insoluble surfactants. Their goal is to find out the possibility to stabilize the effects of the heater located in the wall. This problem has been investigated experimentally and theoretically in the absence of insoluble surfactants by Kabov (1998), Frank (2003), Skotheim et al. (2003), Tiwari and Davis (2009a,b) and Liu and Kabov (2013). Linear and nonlinear instabilities are considered. The small wavenumber approximation is used to obtain a Benney-type equation [see Eq. (18)], which in this case is coupled to a nonlinear equation which includes the free surface deformation and the concentration of the insoluble surfactant. The heater is simulated by means of the following function of the temperature of the wall:

$$T_s(x) = \frac{1}{2} \left[ \tanh(x + 4) - \tanh\left(\frac{1}{2}x - 4\right) \right] \quad (21)$$

Notice that this function has the form of a finite plateau whose extension can be controlled with the constants inside the arguments. It is found that the wave amplitude decreases with the surfactant. This effect is in contrast to that of thermocapillarity. In this way, the surfactant has a stabilizing effect because the film thickness at the valley of the wave is larger, avoiding breakup. The linear analysis showed the possibility of stationary and oscillatory modes of instability. These linear results were tested in the non-linear problem and they were found to be in good agreement. It is also observed that the increase of the surfactant diffusivity has a destabilizing effect by not allowing the local surfactant accumulation.

Katkar and Davis (2013) investigate the non-linear stability of a thin film flowing down a finite heater. In this case, the liquid film presents evaporation effects. The problem has been investigated in the papers presented in the previous review. However, the effect of evaporation has been included in the paper by Joo et al. (1991) under the lubrication approximation. A one-dimensional evolution equation of the free surface perturbations is calculated including thermocapillary effects under the lubrication approximation. They add to thermocapillarity and free surface mass flux the

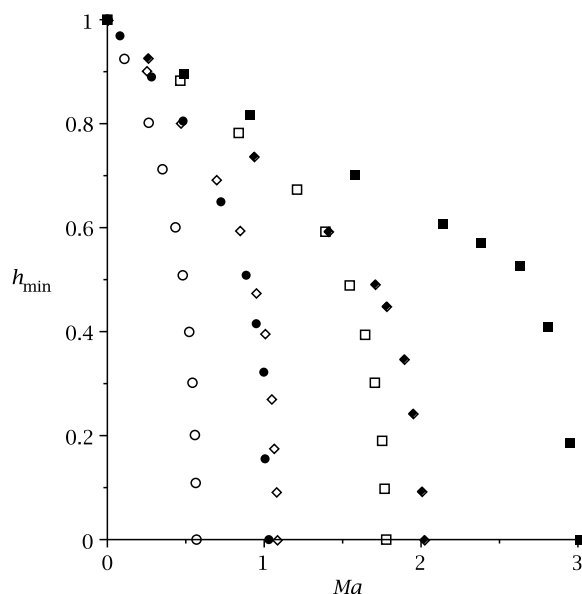


**FIG. 6:** Minimum thickness of the layer  $h_{\min}$  vs Ma. Solid: one heater and void: two heaters. Circles:  $r = 1$ , diamonds:  $r = 4$ , boxes;  $r = 8$ .  $r = l_y/l_x$  is the ratio of the dimensions of each heater.  $Bi = 0$ , Bond number = 10 and the wavelengths are  $L_x = L_y = 40$ .

terms that model the temperature profile in order to simulate a heater of finite length. An equation similar to Eq. (21) is used to this goal. The equation is made non-dimensional in such a way that the Reynolds number, representing the film flow velocity, does not appear explicitly. In this case, Eq. (18) should present an extra term outside the brackets in the form  $T_s(x)Bi/(1 + Bi h)$  multiplied by the evaporation parameter [see Joo et al. (1991)]. An oscillatory mode of instability with hysteresis results. This hysteresis is also found in the case of a non-evaporating film. It depends on the Marangoni number  $Ma$ , representing the strength of thermocapillary effects, as can be seen in Fig. 7 for two evaporation numbers. The oscillations start to appear after a steady stable state for a particular magnitude of  $Ma = Ma_1$ . However, when decreasing the magnitude of  $Ma$ , the oscillatory flow returns to a steady state with smaller  $Ma < Ma_1$ . It is shown in Fig. 7 that the magnitudes of these two Marangoni numbers depend on the evaporation rate. Also, a dependence is found on the Biot number, the heat transfer at the free surface.

### 5.3 Wall Topography

Slade et al. (2013) investigate the rivulet formation from a thin film flowing down a hot or cooled wall with some deformations. Research about fingering instability has been done previously. Examples are the papers by Eres et al. (2000) and Diez and Kondic (2001). Topography of the wall has been taken into account by Zhao and Marshall (2006), Lee et al. (2007), Veremieiev et al. (2010), Sadiq (2013), and by Dávalos-Orozco (2007, 2013, 2014, 2015) (see below). The goal of Slade et al. (2013) is to find out the possibility to have rivulet merging downstream due to a particular topography. The evolution equation is calculated under the small wavenumber approximation including thermocapillary effects. The deformation of the wall is assumed to be two square structures. Each of the square structures is modeled by a function of the form

$$S(x, y) = A \left[ \tan^{-1} \left( \frac{x - B}{D} \right) + \tan^{-1} \left( \frac{-x - C}{D} \right) \right] \left[ \tan^{-1} \left( \frac{y - B_1}{D_1} \right) + \tan^{-1} \left( \frac{-y - C_1}{D_1} \right) \right]. \quad (22)$$

The set of parameters  $A$ ,  $B$ ,  $C$ ,  $D$ ,  $B_1$ ,  $C_1$ , and  $D_1$  are used to control the position of the center and dimensions of the trenches. The set of squares can be two trenches, two peaks and one trench and one peak. The distance between them

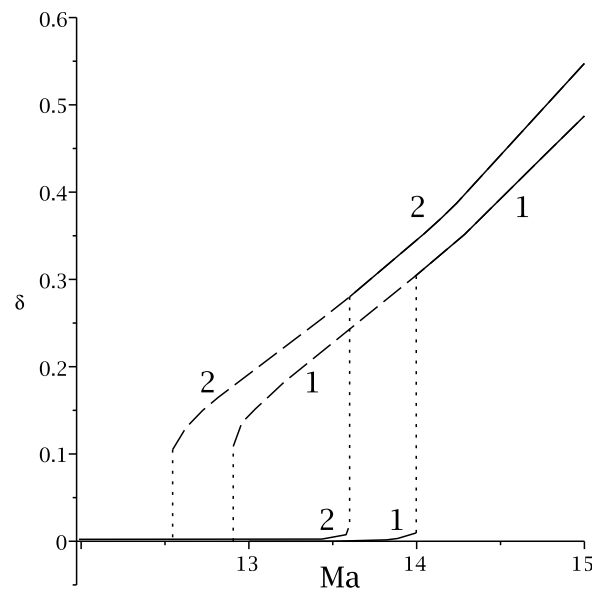


**FIG. 7:** Amplitude of oscillations  $\delta$  vs  $Ma$ . Hysteresis.  $Bi = 0.125$ . Evaporation parameter (1)  $10^{-8}$  and (2)  $10^{-1}$ . Solid:  $Ma$  increases, dashed:  $Ma$  decreases.

also plays an important role in the result. In the flat wall case they show that, when the heating is from below, merging of rivulets is not possible in the space and time investigated. Merging is possible in the isothermal and in the cooled from below case. It is also found that the extension of the rivulets is shorter in the cold wall case. Samples are given for different topographical sets when the wall is cooled from below. In the absence of topography the two rivulets are able to merge. In the presence of two trenches the rivulets cannot merge. When the wall has two peaks the rivulets merge immediately, advancing faster with a longer length than in the other cases. If there are one trench and one peak the rivulets take more time, but finally they can merge. However, the rivulet speed is a little smaller than that of the previous case. This shows the importance of topography in relation with thermocapillary effects on rivulets.

Sadiq (2013) makes calculations of the linear instability of a viscoelastic film flowing down a wall whose deformations are periodic furrows aligned in the direction of the flow. The shear stress tensor satisfies a simplified Walters-B viscoelastic model with very short memory. This viscoelastic model gives a great algebraic simplification because the shear stress tensor has an explicit formula. The thin film stability flowing down a wall with longitudinal furrows has been investigated before by Gambaryan-Roisman and Stephan (2009), Helbig et al. (2009), Sadiq (2012), and Sadiq et al. (2012). The wall is heated uniformly and the free surface of the film suffers thermocapillary effects. A small wavenumber approximation is used to obtain a nonlinear evolution equation of the Benney type which includes thermocapillary and topographic effects. This equation, which has spatially periodic coefficients, is linearized and solved numerically by means of a Chebyshev spectral collocation method. An assumption in the problem is that the wall is vertical in all the calculations. It is found that for strong surface tension and small Reynolds numbers the flow destabilizes when the amplitude of the wall deformation increases. Besides, it is shown that thermocapillarity may have stabilizing effects for moderate strength of surface tension, in a range of amplitudes of wall deformation. Viscoelastic effects are destabilizing in contrast to the stabilization with wall topography. The results demonstrate that this instability is enhanced by an increase of the average flow rate.

Dávalos-Orozco (2014) investigates the stability of a thin film flowing down a heated wall with sinusoidal topography perpendicular to the flow direction. It is assumed that the wall has a finite thickness as shown in Fig. 1. The thickness of the wall without topography is taken into account in Dávalos-Orozco (2012). The isothermal problem with topography was presented by Trifonov (2007a,b, 2014), Scholle et al. (2008), Wierschem et al. (2008, 2010), and Dávalos-Orozco (2007, 2008). The thermocapillary problem was investigated by D'Allesio et al. (2010) using the weighted-residual integral boundary layer model and by Dávalos-Orozco (2013) using the lubrication approximation. The effect of a thick wall with periodic topography in the direction of the flow was taken into account by Gambaryan-Roisman and Stephan (2009). In Dávalos-Orozco (2014) time-dependent periodic perturbations are applied (number 6 in Fig. 1) to the free surface at the origin of the  $x$  direction which is parallel to the main flow. These perturbations propagate superposed to the free surface response (number 4 in Fig. 1) to the wall topography (number 1 in Fig. 1). A nonlinear evolution Eq. (18) is calculated under the small wavenumber approximation. The equation includes the thickness, thermal conductivity, and topography of the wall along with thermocapillary effects. In the absence of time-dependent perturbations the film only presents the free surface response to the wall deformations. It is shown that, when the wall is very thin (Dávalos-Orozco, 2013), the amplitude of the response grows when increasing the Marangoni number. However, in this paper it is demonstrated that, for particular small magnitudes of the relative thickness and thermal conductivity of the wall, the response of the free surface to the sinusoidal wall is able to decrease its amplitude increasing the Marangoni number as seen in Fig. 8. In the figure the frequency of the time-dependent perturbations is  $\omega = 1$  and  $R = 1.967$ . Notice that the mean relative thickness of the wall is very thin,  $d = 0.11$ . The relative magnitude of the wall wavelength over that of the time-dependent perturbations  $L = 9$ . Two magnitudes of the relative thermal conductivity of the wall are used,  $Q_C = 0.01$  and  $0.05$ . In each case, three Marangoni numbers are used,  $Ma = 10, 50, 100$ . It is clear that the amplitude of the response (between  $x = -100$  and  $0$ ) decreases increasing  $Ma$ . That is, going from curves 2 to 4 and from curves 5 to 7. In Fig. 9, for  $L = 6$ , it is shown that even under these conditions it is possible to have resonance to stabilize the perturbations in space and time (see Dávalos-Orozco, 2007, 2013). The reason for the decrease of the thin film response to the wall deformation increasing  $Ma$  is that around the thinnest regions of the wavy wall (the valley) the free surface feels a sudden heating producing a bump, very similar to the one found when a film runs into a finite hot plate, as has been reviewed above in Section 5.2. This bump occurs near the valley of the response which increases its height notably in such a way that the total amplitude of the free surface response is reduced.

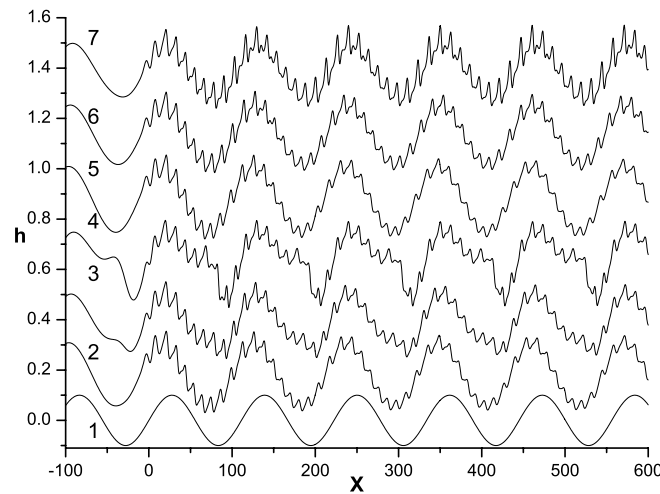


**FIG. 8:**  $Pr = 7$ ,  $S = 1$ ,  $Bi = 0.1$ ,  $d = 0.11$ ,  $\omega = 1$ ,  $R = 1.967$ ,  $L = 9$ . (1) Wall.  $Q_C = 0.01$ : (2)  $Ma = 10$ , (3)  $Ma = 50$ , (4)  $Ma = 100$ .  $Q_C = 0.05$ : (5)  $Ma = 10$ , (6)  $Ma = 50$ , (7)  $Ma = 100$ . Notice pure responses from  $x = -100$  to 0.

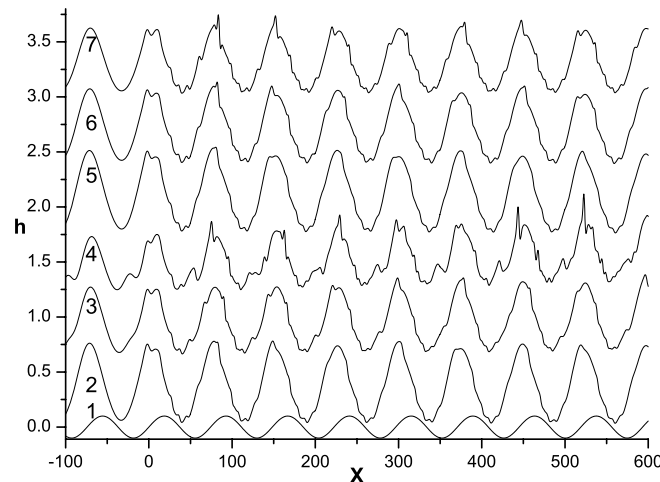


**FIG. 9:** The same as Fig. 8, but  $L = 6$ . The free surface response decreases with  $Ma$ . Resonance. Notice pure responses from  $x = -100$  to 0.

Dávalos-Orozco (2015) investigates the stability of a thin film flowing down a cooled wall. The wall is assumed to have the same physical and geometrical characteristics (see Fig. 1) as in Dávalos-Orozco (2014). However, now the wall is cold and the free surface response feels a sudden and strong cooling at the valleys of the sinusoidal wall. In this case, the response to the wall deformations produces a depression, instead of a bump. This sudden depression is similar to that found when a thin film runs out from a finite hot plate. Therefore, this depression contributes to an increase of the amplitude of the free surface response. When imposing time-dependent perturbations under the conditions of a cooling wall, it is clear that they fade away in space and time. However, it is found that spatial resonance (Dávalos-Orozco, 2007, 2013) is still more efficient to stabilize these perturbations, taking into account that the film response increases its amplitude under the cooling conditions assumed in the paper.

## 6. SOME EXPERIMENTS

In this section papers are discussed which only present experimental results with no proposed theoretical modeling. However, they certainly have experimental and theoretical background. The experiments of some papers use a local heater in the wall. In others the film is already heated uniformly starting from the inlet. Sometimes artificial time-dependent and spatial perturbations are applied near to the inlet. One publication deals with electrostatic forces.

Chinnov (2013) investigates the temperature distribution on the free surface waves of a thin film falling down a vertical wall with a hot plate located a distance from the fluid inlet. Previous research on this subject can be found in Chinnov (2011), Chinnov and Shatskii (2011), Chinnov et al. (2012), and Chinnov and Abdurakipov (2012). Here, the Reynolds number is fixed to a magnitude of 300. The fluorescence and thermal imaging methods are used in this investigation. The goal is to determine the interaction between free surface waves and thermocapillary forces when the film flows down a hot plate with size  $150 \times 100$  mm. The plate is located a distance of 263 mm from the inlet in order to ensure nonlinear saturation of the waves. Longitudinal structures are observed in the mean. They show rivulets with large amplitudes and valleys between the rivulets with small amplitudes distributed periodically in the direction perpendicular to the flow. It is found that the mean film thickness increases in the rivulets and decreases in the valleys while falling down the hot plate. It is also shown that the free surface deformations increase with the heat flux density. In order to understand the role played by the thermocapillary forces, the ratio of the free surface stresses over the wall stresses is used as a modified Marangoni number  $Mn$  as shown in Fig. 10. At the free surface the shear stresses depend on the temperature gradient and the temperature derivative of surface tension. Notice that Fig. 10 only shows the mean value of the data of  $Mn$ . The experimental results show that this Marangoni number increases with the heat flux density in the valleys between rivulets, but remains almost constant in the rivulets.

Rohlfes et al. (2013) investigate the stability of a liquid film flowing down a hot plate in the presence of electrostatic forces. The fluid considered is dielectric and measurements of the local three-dimensional film thickness are done by means of the confocal chromatic imaging method. The background of this paper can be found in Darabi et al. (2000), Tomar et al. (2007), and Rohlfes et al. (2012). The experimental settings are based on Cohen-Sabban et al. (2001) and Dietze and Kneer (2011). Measurements are done for isothermal and non-isothermal flows. The Reynolds number is fixed at 4.5 and the spanwise perturbations, produced by uniformly separated needles, have a wavelength

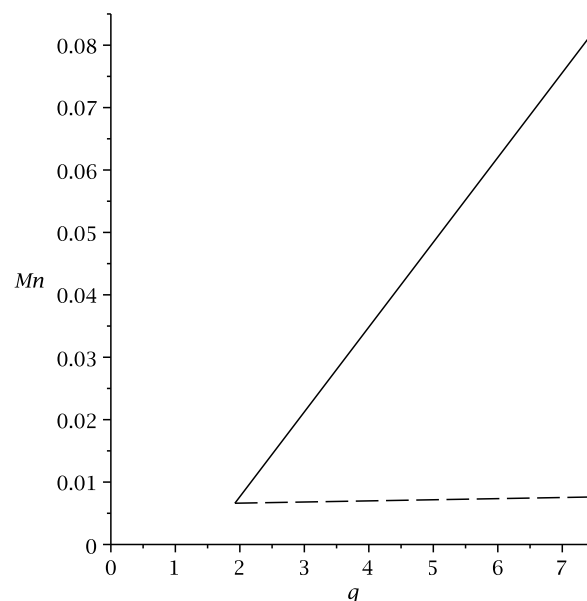


**FIG. 10:** Averaged value of the modified Marangoni number  $Mn$  vs heat flux  $q$  (W/cm<sup>2</sup>).  $R = 300$ . Solid: in the valley between rivulets. Dashed: in the rivulets.

of 30 mm. Besides, time-dependent perturbations are generated by means of a speaker. It is found that the amplitude of the free surface perturbations increases with electrostatic effects in the isothermal case. When the plate is hot, both thermocapillary and electrostatic effects contribute to the increase of the wave amplitude. It is observed that at high frequencies thermocapillarity is less effective and the film velocity increases. However, electrostatic forces always contribute to the formation of rivulets affecting the efficient wall heat dissipation.

Chinnov (2014) investigates the instability of a thin film flowing down a wall with a hot plate of size  $100 \times 150$  mm. It is of particular interest that the Reynolds numbers used are up to 500, larger than that of the previous paper of the author. Here, the distance from liquid inlet to the upper edge of the hot plate is set to 264 mm in order to have saturated waves reaching the plate. Measurements are done using the infrared scanner and the fluorescence method. They are made at different distances from the top of the vertical plate. The review presented here is only for the case of Reynolds number 500. The results show a slight increase of the average distance between rivulets with an increase of the heat flux density. This is seen in Fig. 11 where the averaged distance between rivulets  $D_r$  is plotted against the heat flux  $q$ . There, a comparison of results with  $R = 500$  is done with respect to those of  $R = 300$ . In both cases the distance increase with  $q$  is slow but it is notable when  $R = 500$ . Besides, it is observed that the maximum amplitude of the valleys decreases with the local Reynolds number. In contrast, the amplitude of the rivulets remain almost constant. It is interesting that temperature fluctuations are found near the lower edge of the plate. An example is given for fixed Reynolds number 500 and a heat flux density of  $9.6 \text{ W/cm}^2$ . In this case, at a distance of 100 mm the amplitude of temperature oscillations in the valleys can reach a magnitude of 14 k and in the rivulets of 10 k. However, at a distance of 75 mm the maximum oscillation amplitude is found to be of 20 k.

Rietz et al. (2015) investigate experimentally the pattern formation in thin films falling down a vertical wall with a hot plate  $140 \times 130$  mm. Previous related papers have been published as in Rohlfes et al. (2012) and Rohlfes et al. (2013) (reviewed above). Other experiments have been performed by Kabov et al. (2002) and Lel et al. (2008). The interest is to understand the influence of the heat flux on the free surface topology of the falling film. Three-dimensional waves are observed which have spanwise and streamwise periodicity whose amplitudes growth is enhanced by themocapillarity. In particular, the research is focused on solitary surface waves. In order to know the temperature distribution and film thickness, they use the experimental methods of infrared thermography and chromatic confocal imaging. The upper edge of the hot plate is at 330 mm from the fluid inlet to ensure nonlinear saturation of the waves. This distance comprises a steel plate plus a polyvinyl chloride block with very low thermal conductivity ( $0.20 \text{ w/mK}$ ). The wall-side heat flux is provide by heating cartridges embedded in a thick copper plate. The Reynolds number is fixed to 4.5, the Prandtl number is 167, and the Marangoni number is 3.87. The Kapitza number, representative of surface tension,

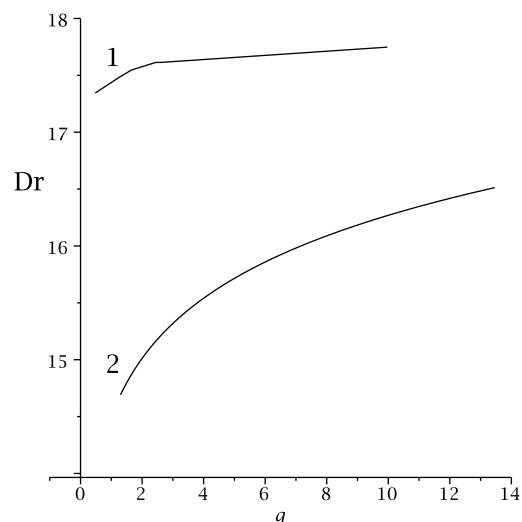


**FIG. 11:** Averaged transverse distance between rivulets  $D_r$  vs heat flux  $q$  ( $\text{W/cm}^2$ ). (1)  $R = 300$ , (2)  $R = 500$ .



is 23.8. Time-dependent perturbations are imposed near the fluid inlet. Besides, spanwise spatial perturbations are generated by five needles uniformly distributed which are in touch of the film. Due to the needles the thin film starts to generate downstream a horseshoe pattern separated by two-dimensional wave fronts. The largest film height appears in front of the horseshoe pattern and the lowest one shows at both sides of this structure. However, thermocapillarity also favors the appearance of two high peaks on both sides of the horseshoe pattern. As a consequence, the film thickness between the peaks decreases considerably, leaving a residual layer and rivulets start to form advancing down the hot plate. Though very thin, the layer thickness between the rivulets increases without saturation in the same way as the peaks. Afterward, secondary rivulets are able to form generating regions of very small thickness. The change of height and the free surface profile in the hot plate might be due to a variation of the viscosity near the plate and to thermocapillary effects. Observations show that after being perturbed by the needles, the film presents characteristics of solitary waves which change with distance into a wave with a secondary structure. The graph in Fig. 12 present plots of the height  $h$  of the advancing film (in micrometers) at different positions in the spanwise  $z$  direction against distance  $x$  (in millimeters) down the hot plate. The data of curves 1 ( $z = 8$  mm), 2 ( $z = 14$  mm), and 3 ( $z = 21$  mm) correspond to the behavior with distance of two maxima (curves 1 and 2) and a valley (curve 3) of the wave. The values of the location in the  $z$ -direction are approximate. As can be seen, the height of the maxima increases and that of the valley decreases with  $x$ . The curves 4 ( $z = 21$  mm), 5 ( $z = 12$  mm), 6 ( $z = 7$  mm), and 7 ( $z = 16$  mm) correspond to data of the residual layer where rivulets are formed. There, the height behavior of two maxima (curves 4 and 5) and two valleys (curves 6 and 7) is plotted against distance down the hot plate. The valley curve 7 is located between the maxima curves 4 and 5. Notice that the curve 6 of the other valley remains almost constant. As can be observed, the height of the film in the residual layer is by far smaller than that of the wave. As in the maxima of the wave, the height of the rivulets maxima in the residual layer increases with distance down the hot plate and that of the valleys decreases with  $x$ .

Markides et al. (2016) combine simultaneously the planar laser-induced fluorescence and infrared thermography imaging to investigate the stability of a thin film flowing down a wall made of an electrically heated titanium foil with a thickness of  $50 \mu\text{m}$  supported by electrodes. The fluorescent dye used is Rhodamine B. This paper follows those of Mathie and Markides (2013) and Mathie et al. (2013). Research using laser-induced fluorescence has been done

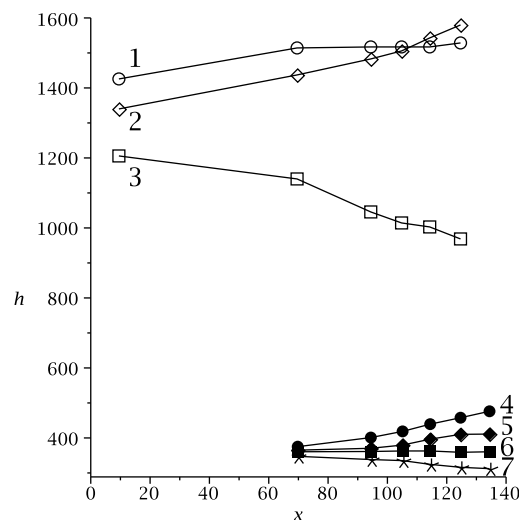


**FIG. 12:** Height  $h$  ( $\mu\text{m}$ ) vs  $x$  (mm). At different positions in the spanwise  $z$  direction and down the hot plate. The data of curves 1 ( $z = 8$  mm), 2 ( $z = 14$  mm), and 3 ( $z = 21$  mm) correspond to the behavior with distance of two maxima (curves 1 and 2) and a valley (curve 3) of the wave. The curves 4 ( $z = 21$  mm), 5 ( $z = 12$  mm), 6 ( $z = 7$  mm), and 7 ( $z = 16$  mm) correspond to data of the residual layer where rivulets are formed. There are two maxima (curves 4 and 5) and two valleys (curves 6 and 7).

by Alekseenko et al. (2012), Morgan et al. (2012), Zadrazil et al. (2014), and by Charogiannis et al. (2015). Infrared thermography is used in Lel et al. (2008) and Zhang et al. (2008a,b). Notice that the simultaneous measurement of the thin film thickness and temperature has been done before by Schagen and Modigell (2007). The goals in Markides et al. (2016) are to measure the film thickness, the free surface temperature, and the heat transfer coefficient. Of importance also are the temperature and heat transfer at the fluid–wall interface. Note that both methods are noninvasive. The liquids used in the experiments were water and water–ethanol solutions (20% and 80%, respectively). The latter has a better wettability, mainly when heating from below. In the experiments the temperature is kept below 40°C to have minimum evaporation. The inclination angle of the wall is selected to be 40° for all the experiments. Measurements are only done at two distances from the liquid inlet. They are  $x = 185$  mm and  $x = 285$  mm, where  $x$  means the main flow direction. Flows for two Reynolds numbers 179 and 251 were investigated. The liquid film heating starts just after it comes out from the inlet, where it begins to form longitudinal structures with cold and hot regions distributed parallel to the main flow. The film is thick in low-temperature regions and thin in high-temperature areas. This is the source of thermocapillary shear stresses in the direction perpendicular to the flow, which as a result lead to the formation of rivulets. It may occur that in a location of the film the temperature difference between the film and the wall is highly reduced. This is interpreted as having a local high heat transfer coefficient. In this paper, the hot plate has a very thin thickness and therefore it is called foil. This allows us to make temperature measurements from the other side of the foil and to take the difference with respect to the temperature of the film in order to calculate the heat transfer coefficient. In some experiments inlet flow pulsations (time-dependent perturbations) are used. They allow us to obtain coherent and higher amplitude film thicknesses fluctuations which lead to better modulated heat transfer coefficient fluctuations. This heat transfer coefficient is found to be higher (by a factor of 3) than that predicted by Nusselt theory (steady, laminar flow). The result is a consequence of the unsteady wavy flow found at high Reynolds numbers. In other words, mixing plays a relevant role to increase the heat transfer coefficient. It is observed that for small Reynolds numbers the experimental results agree very well with Nusselt theory.

## 7. CONCLUSIONS

In this paper a review is given about phenomena taking place in thin films falling down a hot wall. Emphasis is given to situations where the film stability depends on thermocapillarity. Papers containing theoretical and numerical results were presented in the first three sections. Some of the papers of these sections also contain experimental results. The last section is devoted to papers which only report experimental results and novel measurement techniques.

The importance of the temperature dependence of the physical properties of the fluid is reflected in some papers. This assumption gives a better approach to experimental results when the temperature gradient across the layer is large. The temperature dependence of density is also taken into account to include buoyancy effects in the thin-film flow under the Boussinesq approximation. This brings the possibility to calculate a number of main velocity profiles depending on all the physical parameters which vary with temperature.

The substrate not necessarily has a planar geometry. Examples were given where the thin film falls down cylindrical walls. If the cylindrical wall is very thin it is called a fiber. In this case the throttling effects of radial surface tension are very important assisting in the bead formation with the help of thermocapillarity. When the radius of the cylinder is very large with respect to the thickness of the film, it is shown that the axial mode is the most unstable one. However, with the viscoelasticity of the fluid, it is easier to promote the appearance of the azimuthal perturbations. It is shown that thermocapillarity destabilizes the azimuthal modes in such a way that they are able to appear as the more unstable ones in a wide range of perturbation wavenumbers. They can be excited as the more unstable controlling the wavenumber by a suitable frequency of time-dependent perturbations, as done in some papers discussed in this review.

The film can be heated non-uniformly in different ways. One is to impose a temperature gradient along the wall. When there is a two-layer film it is also possible to obtain a number of velocity profiles including buoyancy and thermocapillary effects. Another way to heat non-uniformly is to increase or decrease abruptly the temperature of the wall. When the temperature increases abruptly in the local area of a hot plate, the film presents large-amplitude periodic longitudinal structures which show between them very thin residual films. A third possibility to heat non-uniformly is to change the geometry of the wall. It is shown that this case is related to the second one when the

liquid film feels the abrupt change in geometry of the wall as if it were a sudden increase of the thermocapillary effects.

Some papers were discussed which only publish experimental research. Of great importance is the use of novel technology to investigate, in more detail than before, the free surface patterns and temperature distribution of the film. Research methods were infrared thermography to understand the temperature distribution of the film, chromatic confocal imaging to know the film thickness, and planar laser-induced fluorescence also to describe the local film thickness. It is found, for example, that the temperature increase in the thinnest section of the film between two rivulets may lead to the formation of secondary rivulets. It is shown that rivulets can merge when the film is cooled from below in the presence of particular square topographic wall deformations.

Different research areas have been discussed in the present paper with the restriction that the thin film is affected by thermocapillarity and that it is flowing down a wall. It is our hope that this review may stimulate research in this interesting field.

## ACKNOWLEDGMENTS

The authors would like to thank Cain González, Alberto López, Alejandro Pompa, Raúl Reyes, Ma. Teresa Vázquez, and Oralia Jiménez for technical support.

## REFERENCES

- Alekseenko, S., Cherdantsev, A., Cherdantsev, M., Isaenkov, S., Kharlamov, S., and Markovich, D., Application of a high-speed laser-induced fluorescence technique for studying the three-dimensional structure of annular gas-liquid flow, *Exp. Fluids*, vol. **53**, pp. 77–89, 2012.
- Bekezhanova, V. B. and Rodionova, A. V., Longwave stability of two-layer fluid flow in the inclined plane, *Fluid Dynamics*, vol. **50**, pp. 723–736, 2015.
- Bekezhanova, V. B., Change of the types of instability of a steady two-layer flow in an inclined channel, *Fluid Dynamics*, vol. **46**, pp. 525–535, 2011.
- Benney, D. J., Long waves on liquid films, *J. Math. Phys.*, vol. **45**, pp. 150–155, 1966.
- Birikh, R. V., Thermocapillary convection in a horizontal fluid layer, *J. Appl. Math. Tech. Phys.*, vol. **3**, pp. 69–72, 1966.
- Charogiannis, A., An, J. S., and Markides, C. N., A simultaneous planar laser-induced fluorescence, particle image velocimetry and particle tracking velocimetry technique for the investigation of thin liquid-film flows, *Exp. Therm. Fluid Sci.*, vol. **68**, pp. 516–536, 2015.
- Chinnov, E. A. and Shatskii, E. N., Development of artificial perturbations in a non-isothermal liquid film, *High Temperature*, vol. **49**, pp. 918–923, 2011.
- Chinnov, E. A., Thermal entry length in falling liquid film, *Tech. Phys. Lett.*, vol. **37**, pp. 776–779, 2011.
- Chinnov, E. A., Shatskii, E. N., and Kabov, O. A., Evolution of the temperature field at the three-dimensional wave front in a heated liquid film, *High Temperature*, vol. **50**, pp. 98–105, 2012.
- Chinnov, E. A. and Abdurakipov, S. S., Thermal entry length in a falling liquid film at high Reynolds numbers, *High Temperature*, vol. **50**, pp. 400–406, 2012.
- Chinnov, E. A., Thermocapillary effects in nonisothermal liquid film at high Reynolds numbers, *High Temperature*, vol. **51**, pp. 262–267, 2013.
- Chinnov, E. A., Wave-thermocapillary effects in heated liquid films at high Reynolds numbers, *Int. J. Heat Mass Transfer*, vol. **71**, pp. 106–116, 2014.
- Cohen-Sabban, J. and Gaillard-Groleas, J., and Crepin P. J., Quasi confocal extended field surface sensing, *Proc. of SPIE*, vol. **4449**, pp. 178–183, 2001.
- D'Alessio, S. J. D., Seth, C. J. M. P., and Pascal, J. P., The effect of variable properties on thin film stability, *Phys. Fluids*, vol. **26**, 122105, 2014.
- D'Alessio, S. J. D., Pascal, J. P., Jasmine, H. A., and Ogden, K. A., Film flow over heated wavy inclined surfaces, *J. Fluid Mech.*, vol. **665**, pp. 418–456, 2010.

- Darabi, J., Ohadi, M. M., and Desiatoun, S. V., Falling film and spray evaporation enhancement using an applied electric field, *J. Heat Transfer*, vol. **122**, pp. 741–748, 2000.
- Dávalos-Orozco, L. A., Davis, S. H., and Bankoff, S. G., Nonlinear instability of a fluid layer flowing down a vertical wall under imposed time-dependent perturbations, *Phys. Rev. E*, vol. **55**, pp. 374–380, 1997.
- Dávalos-Orozco, L. A. and You, X. Y., Three-dimensional instability of a liquid layer flowing down a heated vertical cylinder, *Phys. Fluids*, vol. **12**, pp. 2198–2209, 2000.
- Dávalos-Orozco, L. A., Nonlinear instability of thin film flowing down a smoothly deformed surface, *Phys. Fluids*, vol. **19**, 074103, pp. 1–8, 2007.
- Dávalos-Orozco, L. A., Instabilities of thin films flowing down flat and smoothly deformed walls, *Microgravity Sci. Technol.*, vol. **20**, pp. 225–229, 2008.
- Dávalos-Orozco, L. A., The effect of the thermal conductivity and thickness of the wall on the nonlinear instability of a thin film flowing down an incline, *Int. J. Non-linear Mech.*, vol. **47**, pp. 1–7, 2012.
- Dávalos-Orozco, L. A., Stability of thin liquid films falling down isothermal and nonisothermal walls, *Interfacial Phenomena Heat Transfer*, vol. **1**, pp. 93–138, 2013.
- Dávalos-Orozco, L. A., Nonlinear instability of a thin film flowing down a smoothly deformed thick wall of finite thermal conductivity, *Interfacial Phenomena Heat Transfer*, vol. **2**, pp. 55–74, 2014.
- Dávalos-Orozco, L. A., Non-linear instability of a thin film flowing down a cooled wavy thick wall of finite thermal conductivity, *Phys. Letters A*, vol. **379**, pp. 962–967, 2015.
- Dietze, G. F. and Kneer, R., Flow separation in falling liquid films, *Frontiers Heat Mass Transfer*, vol. **2**, 033001, pp. 1–14, 2011.
- Diez, J. A. and Kondic, L., Contact line instabilities of thin liquid films, *Phys. Rev. Lett.*, vol. **86**, pp. 632–635, 2001.
- Ding, Z. J. and Wong, T. N., Stability of a localized heated falling film with insoluble surfactants, *Int. J. Heat Mass Transfer*, vol. **67**, pp. 627–636, 2013.
- Ding, Z. J. and Wong, T. N., Falling liquid films on a slippery substrate with Marangoni effects, *Int. J. Heat Mass Transfer*, vol. **90**, pp. 689–701, 2015.
- Elyukhin, V. A. and Kalimulina, L. A., Nonlinear dispersive waves on the surface of a nonisothermal liquid film, *Izv. Akad. Nauk SSSR, Mekh. Zhidk. Gaza*, vol. **1**, pp. 83–88, 1979.
- Eres, M. H., Schwartz, L. W., and Roy, R. V., Fingering phenomena for driven coating films, *Phys. Fluids*, vol. **12**, pp. 1278–1295, 2000.
- Frank, A. M., 3D numerical simulation of regular structure formation in a locally heated falling film, *Eur. J. Mech. B*, vol. **22**, pp. 445–471, 2003.
- Frank, A. M. and Kabov, O. A., Thermocapillary structure formation in a falling film: Experiment and calculations, *Phys. Fluids*, vol. **18**, 032107, pp. 1–10, 2006.
- Frenkel, A. L., Nonlinear theory of strongly undulating thin films flowing down vertical cylinders, *Europhys. Lett.*, vol. **18**, pp. 583–588, 1992.
- Frenkel, A. L., On evolution equations for thin films down solid surfaces, *Phys. Fluids A*, vol. **5**, pp. 2342–2347, 1993.
- Gambaryan-Roisman, T. and Stephan, P., Flow and stability of rivulets on heated surfaces with topography, *J. Heat Transfer*, vol. **131**, 033101, pp. 1–6, 2009.
- Goussis, D. A. and Kelly, R. E., Effects of viscosity on the stability of film flow down heated or cooled inclined surfaces: Long-wavelength analysis, *Phys. Fluids*, vol. **28**, pp. 3207–3214, 1985.
- Goussis, D. A. and Kelly, R. E., Effects of viscosity variation on the stability of a liquid film flow down heated or cooled inclined surfaces: Finite wavelength analysis, *Phys. Fluids*, vol. **30**, pp. 974–982, 1987.
- Helbig, K., Nasarek, R., Gambaryan-Roisman, T., and Stephan, P., Effect of longitudinal minigrooves on flow stability and wave characteristics of falling liquid films, *J. Heat Transfer*, vol. **131**, 011601, pp. 1–8, 2009.
- Hwang, C.-C. and Weng, C.-I., Non-linear stability analysis of film flow down a heated or cooled inclined plane with viscosity variation, *Int. J. Heat Mass Transfer*, vol. **31**, pp. 1775–1784, 1988.
- Joo, S. W., Davis, S. H., and Bankoff, S. G., Long-wave instabilities of heated falling films: Two-dimensional theory of uniform layers, *J. Fluid Mech.*, vol. **230**, pp. 117–146, 1991.
- Joo, S. W., Davis, S. H., and Bankoff, S. G., A mechanism for rivulet formation in heated falling films, *J. Fluid Mech.*, vol. **321**,

- pp. 279–298, 1996.
- Kabov, O. A., Formation of regular structures in a falling liquid film upon local heating, *Thermophys. Aeromech.*, vol. **5**, pp. 547–551, 1998.
- Kabov, O. A., Scheid, B., Sharina, I. A., and Legros, J. C., Heat transfer and rivulet structures formation in a falling thin liquid film locally heated, *Int. J. Ther. Sci.*, vol. **41**, pp. 664–672, 2002.
- Kabova, Y. O. and Kuznetsov, V. V., Downward flow of a nonisothermal thin liquid film with variable viscosity, *J. Appl. Mech. Tech. Phys.*, vol. **43**, pp. 895–901, 2002.
- Kabova, Y. O., Kuznetsov, V. V., and Kabov, O. A., The effect of mutual location of heaters on the falling film dynamics, *Microgravity Sci. Technol.*, vol. **19**, pp. 53–56, 2007.
- Kalliadasis, S. and Chang, H. C., Drop formation during coating of vertical fibres, *J. Fluid Mech.*, vol. **261**, pp. 135–168, 1994.
- Katkar, H. H. and Davis, J. M., Bifurcation in a thin film flowing over a locally heated surface, *J. Fluid Mech.*, vol. **726**, pp. 656–667, 2013.
- Kim, H., Stability analysis of heated thin liquid film flows with constant thermal boundary conditions, *Korean J. Chem. Eng.*, vol. **16**, pp. 764–773, 1999.
- Lee, Y. C., Thompson, H. M., and Gaskell, P. H., An efficient adaptive multigrid algorithm for predicting thin film flow on surfaces containing localised topographic features, *Comput. Fluids*, vol. **36**, pp. 838–855, 2007.
- Lel, V. V., Kellermann, A., Dietze, G., Kneer, R., and Pavlenko, A. N., Investigations of the Marangoni effect on the regular structures in heated wavy liquid films, *Exp. Fluids*, vol. **44**, pp. 341–354, 2008.
- Liu, R. and Liu, Q. S., Thermocapillary effect on the dynamics of viscous beads on vertical fiber, *Phys. Rev. E*, vol. **90**, no. 3, 033005, pp. 1–11, 2014.
- Liu, R. and Kabov, O. A., Effect of mutual location and the shape of heaters on the stability of thin films flowing over locally heated surfaces, *Int. J. Heat Mass Transfer*, vol. **65**, pp. 23–32, 2013.
- Markides, C. N., Mathie, R., and Charogiannis, A., An experimental study of spatio-temporally resolved heat transfer in thin liquid-film over an inclined heated foil, *Int. J. Heat Mass Transfer*, vol. **93**, pp. 872–888, 2016.
- Mathie, R. and Markides, C. N., Heat transfer augmentation in unsteady conjugate thermal systems — Part I: Semi-analytical 1-D framework, *Int. J. Heat Mass Transfer*, vol. **56**, pp. 802–818, 2013.
- Mathie, R., Nakamura, H., and Markides, C. N., Heat transfer augmentation in unsteady conjugate thermal systems — Part II: Applications, *Int. J. Heat Mass Transfer*, vol. **56**, pp. 819–833, 2013.
- Miladinova, S. and Lebon, G., Effects of non-uniform heating and thermocapillarity in evaporating films falling down an inclined plate, *Acta Mech.*, vol. **174**, pp. 33–49, 2005.
- Moctezuma-Sánchez, M. and Dávalos-Orozco, L. A., Linear three dimensional instability of viscoelastic fluid layers flowing down cylindrical walls, *Microgravity Sci. Technol.*, vol. **20**, pp. 161–164, 2008.
- Moctezuma-Sánchez, M. and Dávalos-Orozco, L. A., Azimuthal instability modes in a viscoelastic liquid layer falling down a heated cylinder, *Int. J. Heat Mass Transfer*, vol. **90**, pp. 15–25, 2015.
- Morgan, R. G., Markides, C. N., Hale, C. P., and Hewitt, F. G., Horizontal liquid-liquid flow characteristics at low superficial velocities using laser-induced fluorescence, *Int. J. Multiphase Flow*, vol. **43**, pp. 101–117, 2012.
- Napolitano, L. G., Plane Marangoni Poiseuille flow of two immiscible fluids, *Acta Astronaut.*, vol. **7**, pp. 461–478, 1980.
- Nayfeh, A. H., *Perturbation Methods*, New York: John Wiley and Sons, 1973.
- Nepomnyashchy, A. A., Simanovskii, I. B., and Legros, J. C., *Interfacial Convection in Multilayer Systems*, New York: Springer, 2006.
- Pascal, J. P., Gonputh, N., and D'Alessio, S. J. D., Long-wave instability of flow with temperature dependent fluid properties down a heated incline, *Int. J. Eng. Sci.*, vol. **70**, pp. 73–90, 2013.
- Prokudina, L. A. and Vyatkin, G. P., Instability of a nonisothermal liquid film, *Doklady Physics*, vol. **43**, pp. 652–654, 1998.
- Prokudina, L. A. and Vyatkin, G. P., Self-organization of perturbations in fluid films, *Doklady Physics*, vol. **56**, pp. 444–447, 2011.
- Prokudina, L. A., Influence of surface tension inhomogeneity on the wave flow of a liquid film, *J. Eng. Phys. Thermophys.*, vol. **87**, no. 1, pp. 165–173, 2014a.
- Prokudina, L. A., Nonlinear evolution of perturbations in a thin fluid layer during wave formation, *J. Exp. Theor. Phys.*, vol. **118**,

- pp. 480–488, 2014b.
- Quan, X. Y., Geng, Y., Yuan, P. F., Huang, Z. Q., and Liu, C. J., Experiment and simulation of the shrinkage of falling film upon direct contact with vapor, *Chem. Eng. Sci.*, vol. **135**, pp. 52–60, 2015.
- Quere, D., Thin films flowing on vertical fibers, *Europhys. Lett.*, vol. **13**, pp. 721–726, 1990.
- Rietz, M., Rohlf, W., Kneer, R., and Scheid, B., Experimental investigation of thermal structures in regular three-dimensional falling films, *Eur. Phys. J. Special Topics*, vol. **224**, pp. 355–368, 2015.
- Rohlf, W., Dietze, G. F., Haustein, H. D., Tselodub, O. Yu., and Kneer, R., Experimental investigation into three-dimensional wavy liquid films under the influence of electrostatic forces, *Exp. Fluids*, vol. **53**, pp. 1045–1056, 2012.
- Rohlf, W., Dietze, G. F., Haustein, H. D., and Kneer, R., Experimental investigation of 3-dimensional wavy liquid films under the coupled influence of thermo-capillary and electrostatic forces, *Eur. Phys. J. Special Topics*, vol. **219**, no. 1, pp. 111–119, 2013.
- Ruyer-Quil, C. and Manneville, P., Improved modeling of flows down inclined planes, *Eur. Phys. J. B*, vol. **15**, pp. 357–369, 2000.
- Ruyer-Quil, C. and Manneville, P., Further accuracy and convergence results on the modeling of flows down inclined planes by weighted-residual approximations, *Phys. Fluids*, vol. **14**, pp. 170–183, 2002.
- Sadiq, I. M. R., First-order energy-integral model for thin Newtonian liquids falling along sinusoidal furrows, *Phys. Rev. E*, vol. **85**, 036309, pp. 1–13, 2012.
- Sadiq, I. M. R., Influence of temperature gradient on the stability of a viscoelastic film with gradually fading memory over a topography with ridges and furrows, *Chinese J. Eng.*, Article ID **751909**, pp. 1–21 (open access), 2013.
- Sadiq, I. M. R., Gambaryan-Roisman, T., and Stephan, P., Falling liquid films on longitudinal grooved geometries: Integral boundary layer approach, *Phys. Fluids*, vol. **24**, 014104, pp. 1–20, 2012.
- Schagen, A. and Modigell, M., Local film thickness and temperature distribution measurement in wavy liquid films with a laser-induced luminescence technique, *Exp. Fluids*, vol. **43**, pp. 209–221, 2007.
- Scheid, B., Ruyer-Quil, C., Thiele, U., Kabov, O., Legros, L., and Colinet, P., Validity domain of the Benney equation including the Marangoni effect for closed and open flows, *J. Fluid Mech.*, vol. **527**, pp. 303–335, 2005.
- Scholle, M., Haas, A., Aksel, N., Wilson, M. C. T., Thompson, H. M., and Gaskell, P. H., Competing geometry and inertial effects on local flow structure in thick gravity-driven fluid film, *Phys. Fluids*, vol. **20**, 123101, pp. 1–10, 2008.
- Shlang, T. and Sivashinsky, G. I., Irregular flow of a liquid film down a vertical column, *J. Phys. (France)*, vol. **43**, pp. 459–466, 1982.
- Skotheim, J., Thiele, U., and Scheid, B., On the instability of a falling film due to localized heating, *J. Fluid Mech.*, vol. **475**, pp. 1–19, 2003.
- Slade, D., Veremieiev, S. Lee, Y. C., and Gaskell, P. H., Gravity-driven thin film flow: The influence of topography and surface tension gradient on rivulet formation, *Chem. Eng. Proc.*, vol. **68**, pp. 7–12, 2013.
- Tiwari, N. and Davis, J., Linear stability of a volatile liquid film flowing over a locally heated surface, *Phys. Fluids*, vol. **21**, 022105, pp. 1–19, 2009.
- Tiwari, N. and Davis, J., Nonmodal and nonlinear dynamics of a volatile liquid film flowing over a locally heated surface, *Phys. Fluids*, vol. **21**, 102101, pp. 1–14, 2009.
- Tomar, G., Gerlach, D., Biswas, G., Alleborn, N., Sharma, A., Durst, F., Welch, S., and Delgado, A., Two-phase electrohydrodynamic simulations using a volume-of-fluid approach, *J. Computat. Phys.*, vol. **227**, pp. 1267–1285, 2007.
- Trifonov, Y. Y., Stability and nonlinear wavy regimes in downward film flows on a corrugated surface, *J. Appl. Mech. Tech. Phys.*, vol. **48**, pp. 91–100, 2007a.
- Trifonov, Y. Y., Stability of a viscous liquid film flowing down a periodic surface, *Int. J. Multiphase Flow*, vol. **33**, pp. 1186–1204, 2007b.
- Trifonov, Y. Y., Stability of a film flowing down an inclined corrugated plate: The direct Navier-Stokes computations and Floquet theory, *Phys. Fluids*, vol. **26**, 114101, pp. 1186–1204, 2014.
- van Dyke, M., *Perturbation Methods in Fluid Mechanics*, California: The Parabolic Press, 1975.
- Veremieiev, S., Thompson, H. M., Lee, Y. C., and Gaskell, P. H., Inertial thin film flow on planar surfaces featuring topography, *Comput. Fluids*, vol. **39**, pp. 431–450, 2010.
- Wierschem, A., Bontozoglou, V., Heining, C., Uecker, H., and Aksel, N., Linear resonance in viscous films on inclined wavy planes, *Int. J. Multiphase Flow*, vol. **34**, pp. 580–589, 2008.
- Wierschem, A., Pollak, C., Heining, C., and Aksel, N., Suppression of eddies in films over topography, *Phys. Fluids*, vol. **22**,

113603, pp. 1–8, 2010.

Zadrazil, I., Matar, O. K., and Markides, C. N., An experimental characterization of downwards gas-liquid annular flow by laser-induced fluorescence: Flow regimes and film statistics, *Int. J. Multiphase Flow*, vol. **60**, pp. 87–102, 2014.

Zhang, F., Tang, D. L., Geng, J., and Zhang, Z. B., Study on the temperature distribution of heated falling liquid films, *Physica D*, vol. **237**, pp. 867–872, 2008a.

Zhang, F., Wu, Y. T., Geng, J., and Zhang, Z. B., An investigation of falling liquid films on a vertical heated/cooled plate, *Int. J. Multiphase Flow*, vol. **34**, pp. 13–28, 2008b.

Zhao, Y. and Marshall, J. S., Dynamics of driven liquid films on heterogeneous surfaces, *J. Fluid Mech.*, vol. **559**, pp. 355–378, 2006.